

REPORT OF THE SUBGROUP ON THE TOP QUARK*

R. M. Barnett,^(j) A. Bay,⁽ⁱ⁾ P. Bhat,^(h) K. Cahill,^(l) A. Barbaro Galtieri,^(j) W. Giele,^(h) J. F. Gunion,^(f)
H. E. Haber,^(g) I. Hinchliffe,^(j) B. Hubbard,^(g) R. Kauffman,^(b) S. Klein,^(e) H. Ma,^(d) B. Margolis,^(k)
L. Nodulman,^(m,b) F. Paige,^(d,m) A. Palounek,^(j) A. Para,^(h) R. Partridge,^(e) R. Thun,^(m) H.-J. Trost,^(b)
H. Trottier,^(k) K. Wacker,^(a) C.-P. Yuan^(b)

(a) RWTH Aachen, (b) Argonne National Lab, (c) Boston University, (d) Brookhaven National Lab,
(e) Brown University, (f) University of California Davis, (g) University of California Santa Cruz, (h) Fermilab,
(i) University of Geneva, (j) Lawrence Berkeley Lab, (k) McGill University, (l) University of New Mexico,
(m) Superconducting Super Collider Lab

ABSTRACT

The top group studied discovery issues at the Tevatron as well as measurements to be made at LHC and SSC. Mass measurements, branching ratios, distributions and other issues were studied.

1 Introduction

The Snowmass top subgroup was a part of both the Tevatron and high luminosity (SSC/LHC) groups. There was considerable activity on the part of SSC collaborations, particularly SDC, EMPACT and TEXAS, in preparing answers to PAC questions on top mass and branching measurements, and the results quoted here are perhaps a sampling of that. In addition, possibilities for studying decay angular distributions as well as other physics possibilities will be reported.

The particular results compiled in this report result largely from the efforts of Partridge on discovery issues, Barnett, Gunion, Hubbard, Ma, Klein, Nodulman, Bay, Galtieri and Palounek for top mass, Kauffmann on distributions, Barnett, Gunion, Haber, Hinchliffe, Hubbard and Trost for (Higgs) decays and branching fractions, Paige, Nodulman and Thun on top as background, and Trottier and Margolis for heavy quark neutral current physics.

2 Top Discovery at the Tevatron Collider

The Tevatron Collider is well positioned to discover the top quark if Standard Model predictions hold. Current bounds on the top quark mass are $m_t \geq 89$ GeV from CDF [1] and $m_t \leq 200$ GeV from Standard Model fits to the W and Z masses and Z partial widths.[2] In what follows, we explore the ability of the Tevatron Collider, with luminosity upgrades, to find top for masses up to 200 GeV.

The predominant decay mode of top is expected to be $t \rightarrow Wb$. Thus, the signature for $p\bar{p} \rightarrow t\bar{t}$ is a pair of W 's and a pair of b quarks. To reduce backgrounds, at least one W must be tagged in a leptonic decay mode. The double-tag process where both W 's decay in leptonic channels were well studied at the Breckenridge Workshop [3] and will not be studied here. The double-tag decays into $e\mu$ final states are particularly clean, have little background, and appear to be limited only by their production rate. Single-tag modes identify one W using a lepton + missing E_T signature and require detection of two or more jets in the final state. The single-tag modes have the advantage of a much higher production rate, but must cope with a QCD W + jets background.

In principle, the single-tags should have a lepton + 4 jet topology. However, for low top masses, the b -quark jets typically have small E_T and are difficult to detect. Figure 1 shows the mean E_T for b -quarks originating from top decay obtained using the PYTHIA Monte Carlo program. The combination of low E_T for the b -quark jets and a substantial W + 2 jet background suggests that the double-tag modes are most promising for $m_t \approx 100$ GeV. For higher top quark masses, the b -quark jets have substantial E_T and should be detectable. In particular, the lepton + 4 jet topology allows complete reconstruction of the event and should have substantially smaller backgrounds than the 2 or 3 jet topologies. With sufficient statistics, it should also be possible to make a direct measurement of the top mass.

To study detection of the b -quark jets in top events, the PYTHIA Monte Carlo program is used to generate event samples for various top masses. Single-tag events are selected by requiring $W \rightarrow e\nu_e$ or $W \rightarrow \mu\nu_\mu$ with $E_T(l) > 20$ GeV, $|\eta_l| < 2$ and a neutrino with $E_T(\nu) > 20$ GeV. The b -quark jets are assumed to be identified if they have $|\eta_b| < 3$ and pass an E_T cut of 20 or 25 GeV. Figure 2 shows the acceptance for events with 1 or 2 b -quarks satisfying the pseudorapidity and E_T cuts. The

*Work supported in part by the U. S. Department of Energy, Division of High Energy Physics, Contract W-31-109-ENG-38.

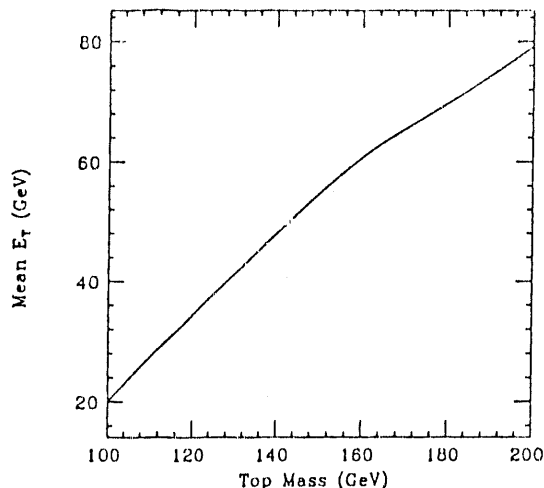


Figure 1: The mean E_T of b quarks from top decay at the Tevatron.

acceptance includes the $W \rightarrow l\nu$ branching ratio but does not include the acceptance for detecting the jets from W decay. These results indicate that there is a rather steep threshold for detecting b -quark jets, with very small probability in the region of the present mass limits increasing to nearly full acceptance for $m_t \approx 130$ GeV.

To estimate the discovery reach of the Tevatron Collider program, it is assumed that there will be collider runs in 1991, 1993, and 1995 with integrated luminosities of 25 pb^{-1} , 50 pb^{-1} , and 250 pb^{-1} , respectively. It is assumed that 10 events are required for discovery and that the cumulative sample from all running periods is used. The discovery reach of lepton + 4 jets is obtained by normalizing to the lepton + 3 jet results from Breckenridge and assuming a 50% inefficiency in finding the fourth jet. The discovery reach for the lepton + 4 jet mode is shown in Table 1, along with the Breckenridge results for the the double-tag $e\mu$ mode. While the discovery reach of the lepton + 4 jet mode is slightly higher than the $e\mu$ mode, both should be detectable if the top-quark lies below ≈ 200 GeV and the assumed luminosities are achieved. Detecting both modes provides an important check on the experimental technique as well as testing the prediction for the top semi-leptonic branching ratio, which is sensitive to non-standard decay modes.

3 Measuring the Top Mass

Three techniques have been studied for measuring the top mass; using decays to all jets, a lepton and a

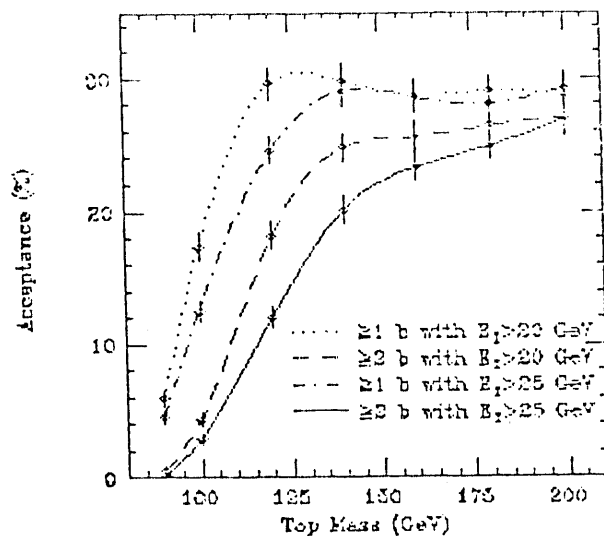


Figure 2: Acceptance for lepton plus 4 jet top events at the Tevatron.

Year	Luminosity	$e\mu$	$l + 4 \text{ jets}$
1991	25 pb^{-1}	$\approx 120 \text{ GeV}$	$\approx 120 \text{ GeV}$
1993	75 pb^{-1}	$\approx 150 \text{ GeV}$	$\approx 160 \text{ GeV}$
1995	325 pb^{-1}	$\approx 190 \text{ GeV}$	$> 200 \text{ GeV}$

Table 1: Discovery Reach for Top

tagged b jet, and 2 leptons. We report first a technique to accurately determine the top quark mass by reconstructing the mass of the three jets from top quark decays. We are interested in $t\bar{t}$ events in which the top quarks decay via $t \rightarrow Wb$ followed by one W decaying to $l\nu$ while the other W decays to two jets. In this Monte Carlo study, which has employed Isajet 6.31, we have taken the top quark mass to be $150 \text{ GeV}/c^2$ and have used the efficiencies and resolutions of the Solenoidal Detector Collaboration (SDC). We trigger by requiring an isolated electron or muon (ℓ) with $p_T > 40 \text{ GeV}/c$ and $|\eta| < 2.5$. The efficiency for this trigger is $e_{\ell\text{-trig}} \approx 0.5$. We further demand two tagged b -jets with $p_T > 30 \text{ GeV}/c$ within $|\eta| < 2.0$. The efficiency for tagging both the b -jets through secondary vertices [4] is $e_{b\text{-tag}} \approx 0.07$ (including the above-mentioned transverse momentum and rapidity requirements). With these trigger and tagging efficiencies, the number of $t\bar{t}$ events per SSC year, $N_{t\bar{t}}$, is reduced to $2N_{t\bar{t}}B(W \rightarrow l\nu)e_{\ell\text{-trig}}e_{b\text{-tag}} = 1.3 \times 10^6$.

Next we attempt to identify the two non- b jets coming from the hadronic decay sequence, $t \rightarrow bW \rightarrow bud$ (or $b\bar{c}\bar{s}$), of the top quark opposite the trigger. Jets are

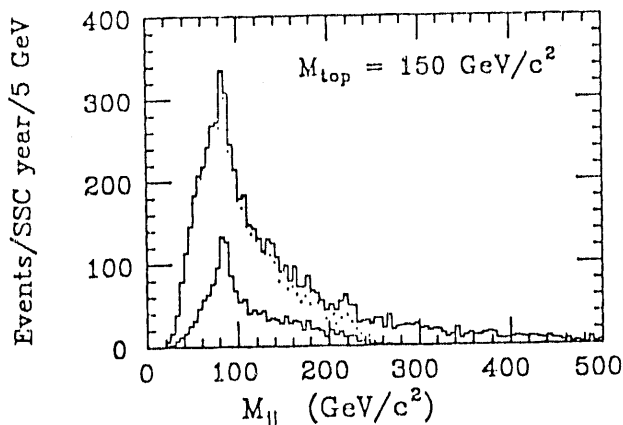


Figure 3: The invariant mass distribution for non- b dijet combinations, for $t\bar{t} \rightarrow WWb\bar{b}$ events. All two-jet combinations are included in the top histogram, while only those consistent with $m(\text{dijet} + b) < 300 \text{ GeV}/c^2$ are plotted in the middle histogram. The bottom histogram retains only the *highest transverse momentum* (see text) jet pairs with $m(\text{dijet} + b) < 300 \text{ GeV}/c^2$.

formed by clustering final-state particles appearing in the region $|\eta| < 3.0$ within a cone of radius $R < 0.6$. The 4-momenta of these jets are then smeared with the jet resolution $\sigma/E = 70\%/\sqrt{E} + 3\%$. Any two non- b jets within $|\eta| < 2.5$ and having $p_T > 20 \text{ GeV}/c$ are then used to form invariant mass combinations. Most events will contain additional jets due to initial- and final-state radiation. We find using Isajet that the average number of non- b jets reconstructed with $|\eta| < 2.5$ and $p_T > 20 \text{ GeV}/c$ is about 3.1. If one examines the invariant mass distributions for all pairs of non- b jets in our events in an attempt to see the mass peak from the hadronic W decays, a substantial combinatoric background is evident, as illustrated in Fig. 3, arising primarily from dijet selections in which one or both of the jets arise from the secondary radiation processes. The relative number of non- $t\bar{t}$ events from continuum production of $Wb\bar{b}$ jet jet selected by the trigger and passing the additional requirements has been found to be well less than a tenth of a percent.[5] A very effective technique for reducing this combinatoric background is to first consider only pairs of non- b jets that in combination with one of the tagged b jets yield a net three-jet invariant mass smaller than $300 \text{ GeV}/c^2$. Of course if we found a mass peak close to $300 \text{ GeV}/c^2$, we would modify this choice. This cut will eliminate a significant number of incorrect combinatoric choices involving radiatively generated jets or the wrong b jet. The two-jet mass distribution after this cut is compared to that before the cut in Fig. 3. As is evident

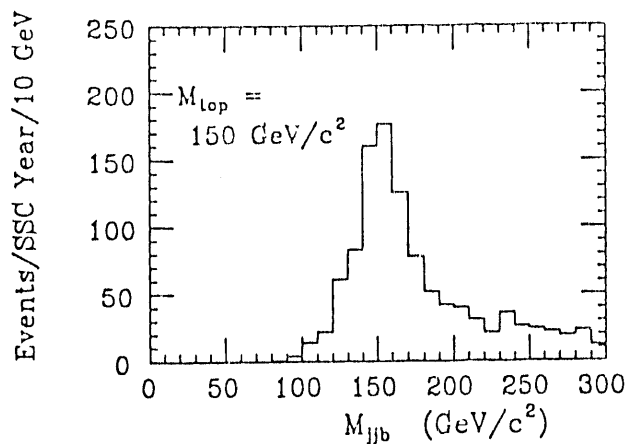


Figure 4: We plot the 3-jet invariant mass distribution, where two of the jets are the ‘highest transverse momentum’ non- b jets with dijet mass in the W mass interval, and the third jet is a tagged b jet. The number of events generated for this plot is less than 1% of that expected for a standard 10^4 pb^{-1} SSC year.

from the figure, the effect of this requirement is to remove much of the combinatoric background present at the high end of the spectrum. Next we restrict our dijet invariant mass plot to the two (non- b) jets with the highest transverse momenta and with $m(3\text{-jet}) < 300 \text{ GeV}/c^2$, where (as before) the third jet is either of the b jets. By “highest transverse momentum”, we mean an algorithm in which we chose the leading p_T jet, and then searched for the remaining jet with the highest p_T such that the 3-jet mass was less than $300 \text{ GeV}/c^2$. If none satisfied this criterion, we began with the next-to-leading jet and again searched the remaining jets (and so on). This distribution is also plotted in Fig. 3. The combinatoric background has been severely reduced by only plotting one combination per event, and the above choice tends to be the correct one.

Finally, to reconstruct the top quark mass we take all events in the W mass interval of the bottom histogram of Fig. 3 ($60 < M_{jj} < 100 \text{ GeV}/c^2$). The two jets used to plot the dijet invariant mass are then combined (separately) with each of the tagged b jets, and the invariant mass of the dijet- b combination is computed. Because of our procedure, the 3-jet mass is guaranteed to lie below $300 \text{ GeV}/c^2$ for at least one of the b -jet choices. The resulting 3-jet invariant mass distribution is plotted in Fig. 4. A remarkably sharp mass peak is evident, centered about the top quark mass of $150 \text{ GeV}/c$. Because of the large number of events retained by this procedure, and the reduction of the combinatoric background by our techniques, we find

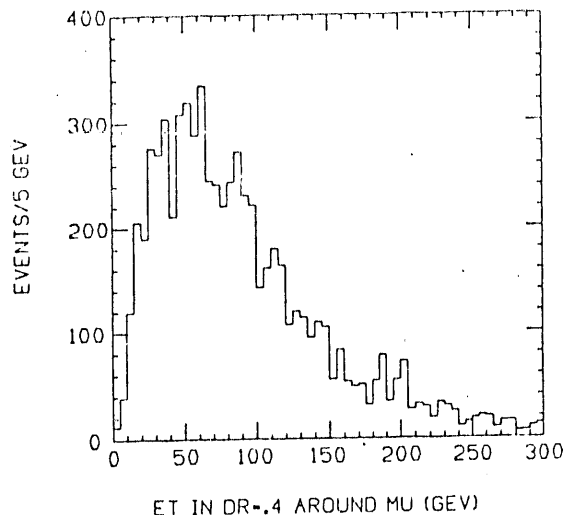


Figure 5: Transverse energy in an $\eta - \phi$ cone of 0.4 around the muon from semileptonic decays of b quarks coming from decays of $250 \text{ GeV}/c^2$ t quarks in simulated SSC events.

that the top mass can be determined statistically to within $\pm 75 \text{ MeV}/c^2$. The actual accuracy of this measurement is limited by systematic errors due primarily to the energy measurement of jets. Assuming that one will do somewhat better than the CDF experiment, we might expect $\pm 2\text{-}3\%$ accuracy ($\pm 3\text{-}4 \text{ GeV}/c^2$).

A different approach is to avoid inherent uncertainties involved in reconstruction using jets and take advantage of the copious rates for top production by using the leptons in semileptonic decays. A typical strategy would be to combine an isolated electron or muon with an opposite sign non-isolated muon. In the process $t \rightarrow Wb$, leptonic decay of the W yields isolated leptons while semileptonic decay of the b yields leptons associated with jets, see Figure 5. Isolation can be conservatively taken to be $10 \text{ GeV } E_T$ in an $\eta - \phi$ cone of radius 0.4. In order to avoid background and wrong combinations, the net p_T of the pair of leptons may be required to be high, say above $100 \text{ GeV}/c$, and each will be high enough to satisfy a dilepton trigger. The sensitivity of such a lepton pair mass to the assumed top mass is shown in Fig. 6. In a standard SSC year, the statistical error for such a distribution is readily less than $\pm 1\%$. These distributions have some sensitivity to the p_T distribution of the parent t quarks, and this will need to be constrained by modeling the distribution of the p_T of the pair of leptons for a given acceptance and cuts. Assuming such an analysis works well, the leading systematic error in determining the t quark mass will come from the fragmentation uncer-

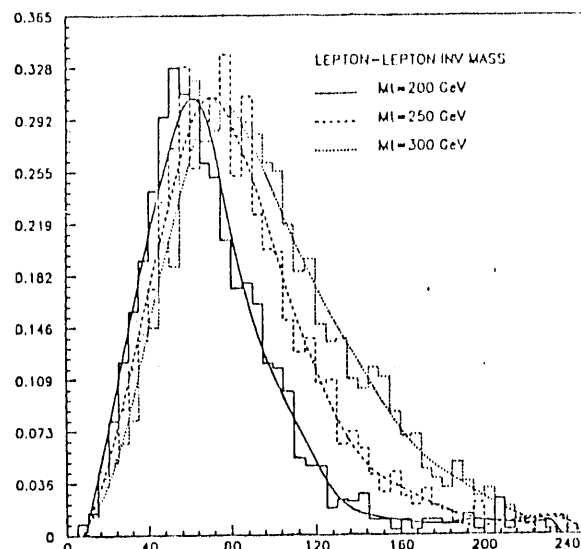


Figure 6: Lepton-lepton invariant mass distribution (in GeV/c^2). The vertical scale is arbitrary yield. The first lepton is the isolated lepton and the second is associated with a jet. Charm decay contamination is considered and the b/c ratio is about 2:1. The curves on the plot are spline fits to illustrate the top mass effect.

tainty for the b quark. Although the t quark decays essentially immediately, the b quark fragmentation needs to be taken into account. The current measurement by ALEPH [6] determines the average muon momentum fraction to $\pm 3\%$. Assuming that improved measurements are diluted by the need to extrapolate so that the average muon momentum fraction can be predicted to $\pm 4\%$, the resulting systematic error on the top mass is then $\pm 2\%$. Detector resolution for the electrons and muons is not particularly relevant.

The need to model the parent p_T distribution as well as the sensitivity to fragmentation may be greatly reduced by combining isolated leptons with tagged b jets. Once again the statistical accuracy in one year at SSC is less than $\pm 1\%$. Such a distribution is shown in Fig. 7, where the b -jet is assumed to be tagged by a vertex detector such that the sign of the b is not determined. This technique involves the systematic error in measuring the energy of a b -jet calorimetrically.

4 Distributions

The latest limit from CDF places the top quark mass above 89 GeV [1] so that it invariably decays into a bottom quark plus a real W boson. With this decay channel open the top quark decays quickly such that a measurement of its lifetime would be very difficult.

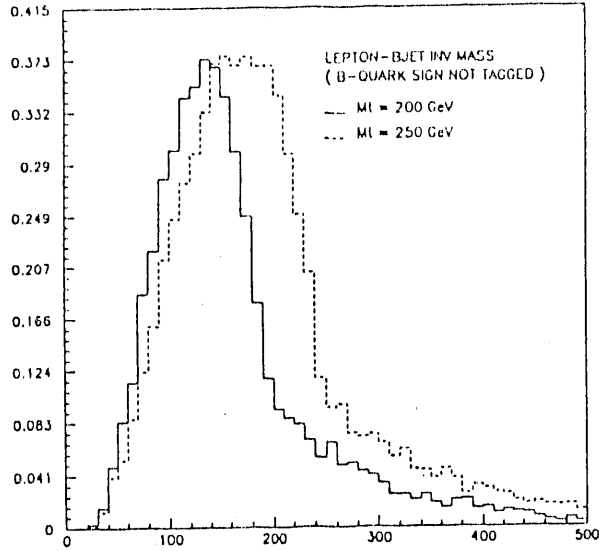


Figure 7: The invariant mass (in GeV/c^2) of an isolated lepton with a b -jet, identified by vertex detector tagging. There is no sign determination for the b quark. All combinations are included. The vertical scale is arbitrary yield.

For a quantity which is measurable and probes the top quark couplings and the dynamics of top quark decay one is led to consider the polarization distribution of the W 's produced in the decay.[7] In the Standard Model the coupling $t \rightarrow b + W$ has the familiar $V - A$ form:

$$\mathcal{M}^\mu = ig_L \bar{u}(b) \gamma^\mu (1 - \gamma^5) u(t),$$

with $g_L = g/2\sqrt{2}$. This leads to the following partial widths for the three helicities of the W :

$$\begin{aligned} \Gamma_- &= \frac{G_F |p|}{2\pi\sqrt{2}} \frac{M_W^2}{m_t} (E_b + |p|) \\ \Gamma_+ &= \frac{G_F |p|}{2\pi\sqrt{2}} \frac{M_W^2}{m_t} (E_b - |p|) \\ \Gamma_0 &= \frac{G_F |p|}{2\pi\sqrt{2}} \left(2|p|^2 + \frac{M_W^2}{m_t} E_b \right), \end{aligned}$$

where E_b is the energy of the b quark in the top quark rest frame and $|p|$ is its momentum:

$$\begin{aligned} E_b &= \frac{1}{2m_t} (m_t^2 - M_W^2 + m_b^2), \\ |p| &= \sqrt{E_b^2 - m_b^2}. \end{aligned}$$

When $E_b \gg m_b$ the right-handed helicity partial width vanishes as can be seen from angular momentum arguments. Notice also that at very large masses, $m_t \gg M_W$, the longitudinal width dominates, being enhanced

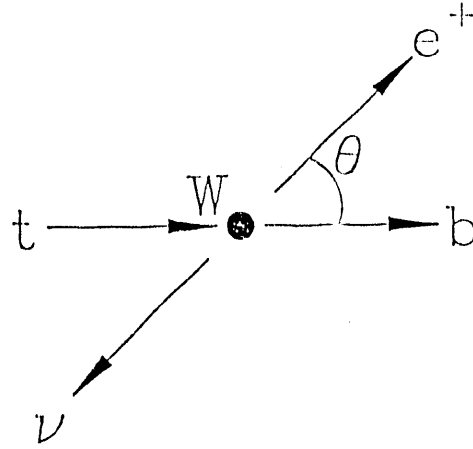


Figure 8: Top quark decay as viewed in the rest frame of the W .

by a factor $(m_t/M_W)^2$ relative to the transverse width. This enhancement is exactly that expected from the Equivalence Theorem which says that the longitudinal W behaves like a scalar at high energies.

The relative widths for the three polarizations are reflected in the angular decay distribution of the W . For simplicity say the W decays into positron plus neutrino. If we define θ as the angle between the positron and the b quark in the W rest frame (see Figure 8) then:

$$\begin{aligned} \frac{d\Gamma_-}{d\cos\theta} &= \frac{3}{8}(1 + \cos\theta)^2, \\ \frac{d\Gamma_+}{d\cos\theta} &= \frac{3}{8}(1 - \cos\theta)^2, \\ \frac{d\Gamma_0}{d\cos\theta} &= \frac{3}{4}(1 - \cos^2\theta). \end{aligned}$$

The distribution in $\cos\theta$ for several values of the top mass is shown in Figure 9. Notice that the shape of the distribution is highly dependent on m_t .

Consider the situation in hadronic production of $t \bar{t}$. A direct measurement of $\cos\theta$ is not possible since it is defined in the rest frame of the W . Transforming to that frame requires a knowledge of the neutrino's momentum. The transverse momentum of the neutrino can be extracted from missing \mathbf{p}_T , up to experimental resolution. The constraint that the positron and neutrino form a W gives two solutions for the neutrino's longitudinal momentum. This ambiguity, as well as the uncertainty in measuring missing \mathbf{p}_T , prevents us from extracting the distribution in $\cos\theta$ directly. An indirect measure of $\cos\theta$, which is unambiguous and does not rely on missing momentum, is the dot prod-

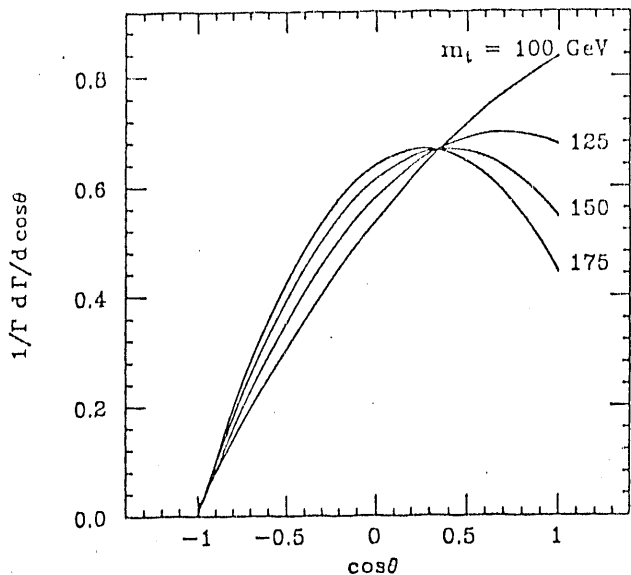


Figure 9: The distribution of events versus $\cos \theta$ for $m_t = 100, 125, 150$ and 175 GeV.

uct of the positron momentum with the b momentum. In the W rest frame write

$$\cos \theta = \frac{1}{|\mathbf{p}_b^{\text{CM}}|} \left(E_b^{\text{CM}} - \frac{2 \mathbf{e} \cdot \mathbf{b}}{M_W^2} \right),$$

where $E_b^{\text{CM}} = (m_t^2 - M_W^2 - m_b^2)/2M_W$ is the b energy, \mathbf{p}_b^{CM} is its momentum and $\mathbf{e} \cdot \mathbf{b}$ is the dot product of the positron and b momenta. Notice that calculating $\cos \theta$ from $\mathbf{e} \cdot \mathbf{b}$ requires knowledge of m_t , since E_b^{CM} depends on it.

This dependence of the extracted value of $\cos \theta$ on the top mass can be inverted to provide a measure of m_t . Imagine a distribution generated with a top mass m_t , but analyzed with the wrong mass m'_t . Let $E_b'^{\text{CM}}$ and $|\mathbf{p}_b'^{\text{CM}}|$ be the W center of mass values for the b energy and momentum appropriate to this wrong mass. Then the apparent value of the cosine, $\cos \theta'$, is expressed in terms of the 'true' $\cos \theta$ as

$$\cos \theta' = \frac{1}{|\mathbf{p}_b'^{\text{CM}}|} (E_b'^{\text{CM}} - E_b^{\text{CM}} + |\mathbf{p}_b^{\text{CM}}| \cos \theta).$$

Thus the distribution with respect to $\cos \theta'$ is

$$\frac{d\Gamma}{d \cos \theta'} = \frac{|\mathbf{p}_b^{\text{CM}}|}{|\mathbf{p}_b'^{\text{CM}}|} \frac{d\Gamma}{d \cos \theta}.$$

The distributions versus $\cos \theta'$ for events generated with $m_t = 150$ GeV but analyzed with $m'_t = 140, 150$ and 160 GeV are shown in Figure 10. We see that the distribution for $m'_t = 140$ GeV extends to values of $\cos \theta'$ less than -1 whereas the distribution

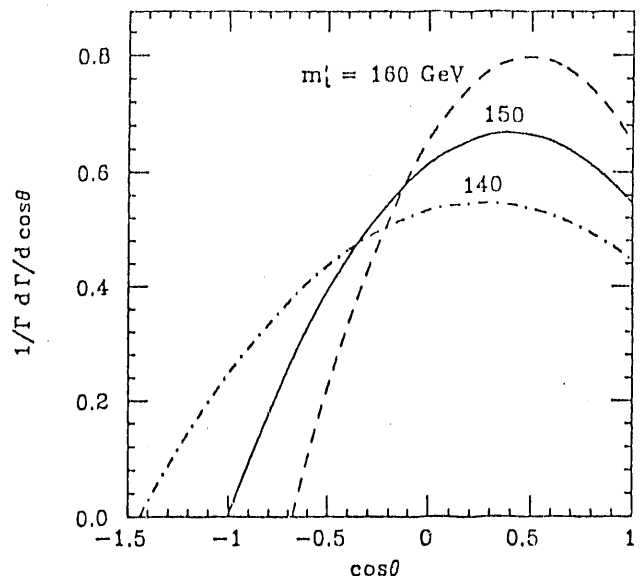


Figure 10: Distribution versus $\cos \theta'$ for events generated with $m_t = 150$ GeV but analyzed with $m'_t = 140, 150$ and 160 GeV.

for $m'_t = 160$ GeV does not cover the full range out to $\cos \theta' = -1$.

When $m'_t < m_t$, a crude measure of the deviation of m'_t from m_t is the fraction of events which have $\cos \theta' < -1$. The point $\cos \theta' = -1$ will correspond to $\cos \theta > -1$:

$$\cos \theta_{\min} = \frac{1}{|\mathbf{p}_b^{\text{CM}}|} (E_b^{\text{CM}} - E_b'^{\text{CM}} - |\mathbf{p}_b'^{\text{CM}}|).$$

If we neglect m_b

$$\cos \theta_{\min} = 1 - 2 \frac{m_t'^2 - M_W^2}{m_t^2 - M_W^2}.$$

The fraction of events with $\cos \theta' < -1$ is

$$f_{\text{under}} = \frac{1}{\Gamma} \int_{-1}^{\cos \theta_{\min}} \frac{d\Gamma}{d \cos \theta'}.$$

This fraction is shown in Table 2 for $m_t = 150$ GeV and various choices for the m'_t . We see even for $m'_t = 149$ GeV there is a 2% effect. However, since we have not included the effect of the finite width of the W ($\Gamma_W \approx 2$ GeV) the analysis as presented here cannot achieve that accuracy.

Although, in principle one event with $\cos \theta < -1$ places a lower bound on the top mass, an analysis of this type will almost certainly be limited by background. Misidentification of the b -quark jet will in general lead to larger values of $\mathbf{e} \cdot \mathbf{b}$ and $\cos \theta < -1$. Therefore it is crucial to obtain a clean sample of tagged

m_t	f_{under}
140	0.218
145	0.106
147	0.063
148	0.042
149	0.021

Table 2: The fraction of events with $\cos \theta' < -1$, for $m_t = 150$ GeV.

events. A straightforward procedure would be to require both top quarks to decay semi-leptonically, the signal being two isolated high- p_T leptons plus two jets. In order to be certain that the two jets are b jets and not gluon jets it is necessary to measure a secondary vertex in both jets. To determine which b goes with which lepton require that one of the b 's decay semi-leptonically, producing a lepton with significant p_T relative to the jet axis. The signs of the charges of the three leptons determine which lepton should be paired with which jet. To obtain optimal resolution one would use the purely hadronic jet to form the desired dot product.

In a canonical SSC year (10^4pb^{-1}) approximately 10^8 top quarks are produced. Requiring two semileptonic decays (into electrons or muons) leaves 5×10^8 . In order to tag the b 's it is necessary to measure the semileptonic decay of one of them, the efficiency of which we estimate to be 0.1. The remaining background would arise from secondary decays of charm mesons leading to a misidentification of the b . A detailed study would be necessary to estimate the significance of this background. It seems reasonable that given the large number of events a mass determination to within ≈ 5 GeV is achievable with this method.

Once the top quark mass is well measured W polarization can be used to test the couplings of the top quark. Consider a top quark which had a right-handed coupling to the W as well as the left-handed coupling of the Standard Model. If we write the current as:

$$\mathcal{M}^\mu = i\bar{u}(b)\gamma^\mu[g_L(1 - \gamma^5) + g_R(1 + \gamma^5)]u(t),$$

then the presence of the right-handed coupling alters the relative proportions of the three polarizations of the W . Define $r = g_R/g_L$. The partial widths are then

$$\Gamma_- = \frac{g_L^2}{2\pi m_t} [E_b + |\mathbf{p}| + r^2(E_b - |\mathbf{p}|) - 2m_b r]$$

$$\Gamma_+ = \frac{g_L^2}{2\pi m_t} [E_b - |\mathbf{p}| + r^2(E_b + |\mathbf{p}|) - 2m_b r]$$

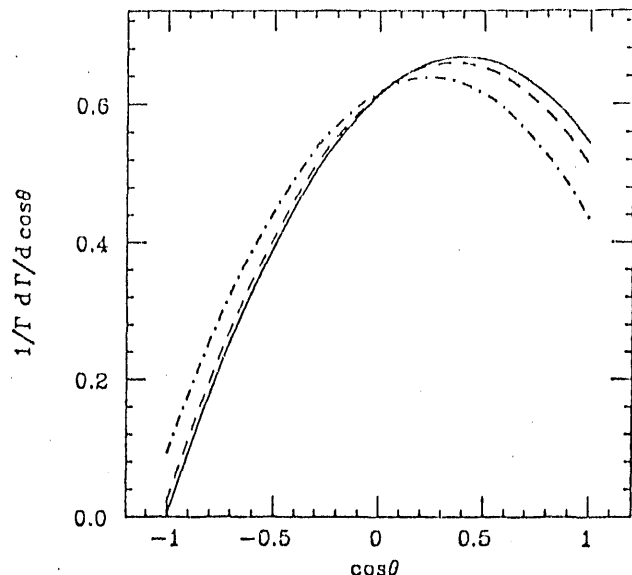


Figure 11: The distribution of events versus $\cos \theta$ for $g_R/g_L = 0$, (solid) $1/4$, (dashed) and $1/2$ (dash dot) with $m_t = 150$ GeV.

$$\Gamma_0 = \frac{g_L^2}{2\pi m_t} \left[(1 + r^2) \left(\frac{2m_t |\mathbf{p}|^2}{M_W^2} + E_b \right) - 2m_b r \right],$$

where E_b and $|\mathbf{p}|$ defined in the top rest frame as before. Notice that the only appreciable effect of $g_R \neq 0$ comes in at second order; the linear interference term is suppressed by m_b . The altered angular distribution caused by the addition of the right-handed coupling is shown in Figure 11. We see that the angular distribution is not very sensitive to small admixtures of right handed coupling.

5 Searching for Top Decays to Charged Higgs Bosons

The high luminosity of hadron colliders will allow a general study of top decay by enabling a large sample of high p_T top events to be cleanly tagged on one side, by the W and b from the t or \bar{t} . The rest of the event may serve as a relatively unbiased top sample. Very clean samples of thousands of events may be obtained, even for top masses of $250 \text{ GeV}/c^2$. Particular decay modes, especially those which may be rare, have their own optimal strategies.

An extension of the standard Higgs sector with two Higgs doublets has both charged and neutral Higgs bosons. If the charged Higgs boson is lighter than the top quark, the branching ratio for the decay $t \rightarrow H^+ b$ could be comparable to that for $t \rightarrow W^+ b$. We use the model of Reference [8]. The branching fractions for $t \rightarrow bH^+$, $H^+ \rightarrow \tau\nu$, and $H^+ \rightarrow c\bar{s}$ (see Fig. 12) are

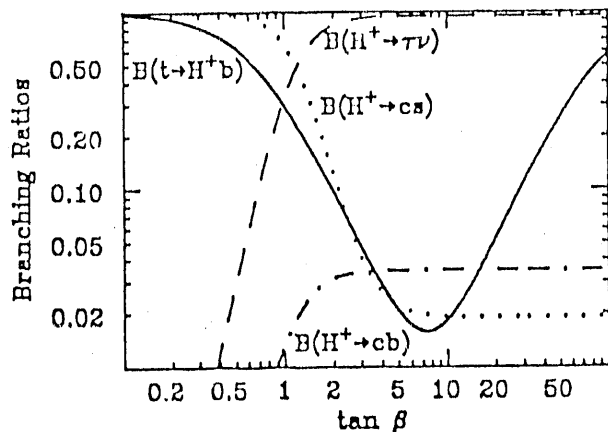


Figure 12: Branching fractions for the reactions $t \rightarrow H^+ b$ (solid) and $H^+ \rightarrow \tau \nu$, $c \bar{s}$, $c \bar{b}$ as a function of $\tan \beta$, see Ref. [8]. We have assumed $m_t = 250 \text{ GeV}/c^2$ and $m_{H^+} = 150 \text{ GeV}/c^2$.

determined by the ratio of vacuum expectation values of the two Higgs doublets, $\tan \beta = v_2/v_1$.

We have investigated two methods for H^+ detection in $t\bar{t}$ events for the case $m_t = 250 \text{ GeV}/c^2$ and $m_{H^+} = 150 \text{ GeV}/c^2$. Method 1 involved a search for an excess of τ leptons. Method 2 involved reconstruction of the hadronic decays $H^+ \rightarrow c \bar{s}$. In each case, events are triggered by requiring one t quark to decay via $t \rightarrow b W^+ \rightarrow b \ell^+ \nu$ yielding an isolated electron or muon (ℓ) with $p_t > 40 \text{ GeV}/c$ and $|\eta| < 2.5$. They are further selected by requiring two tagged b -jets (from the decay of the t and \bar{t}) with $p_t > 30 \text{ GeV}/c$ within $|\eta| < 2.0$. For the $\tau \nu$ and $c \bar{s}$ cases we used ISAJET 6.31; for $\tau \nu$ we duplicated our results with PYTHIA. We have also calculated the non- $t\bar{t}$ background, and in each case it is negligible.

In Method 1 we search for ℓ - τ events (eg, $t \rightarrow b W^+ \rightarrow b \ell^+ \nu$, $\bar{t} \rightarrow \bar{b} H^+ \rightarrow \bar{b} \tau^+ \nu$ or $\bar{b} W^+ \rightarrow \bar{b} \tau^+ \nu$) in which the τ decays to a single π^\pm (or K^\pm) with $p_t > 40$ (or 100) GeV/c . The signature is an isolated charged hadron whose momentum (from tracking) and energy (from calorimetry) agree within errors. If t quarks can only decay to $W^+ b$, then the observed number of $\ell^+ \ell^-$ events plus lepton universality in W decays allows us to compute the number of ℓ - τ events expected. If instead top quarks can also decay to $H^+ b$, we would detect an excess of ℓ - τ events over the universality prediction. This occurs because ℓ - τ events are enhanced, while $\ell^+ \ell^-$ events are depleted.

The statistical significance of the excess in the observed number of isolated pions over the prediction

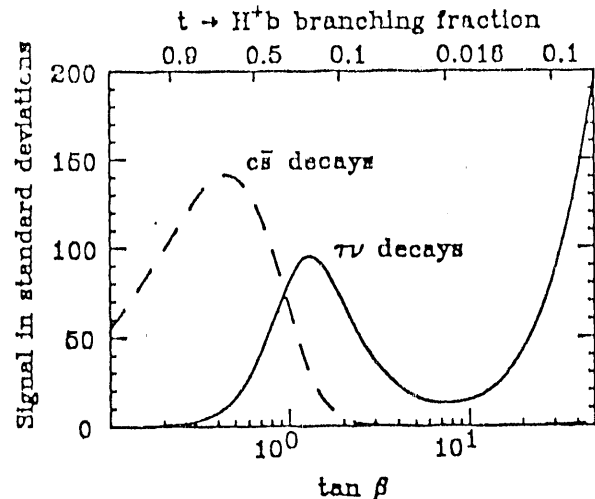


Figure 13: a) Statistical significance (solid curve) of the excess of isolated pions due to $t \rightarrow H^+ b$, $H^+ \rightarrow \tau \nu$, and $\tau \rightarrow \pi \nu$ relative to expectations for $t \rightarrow W^+ b$ (assuming lepton universality) as a function of $\tan \beta$ (bottom labels). We require an isolated lepton with $p_t > 40 \text{ GeV}/c$ and an isolated pion with $p_t > 40 \text{ GeV}/c$ (for $p_t > 100 \text{ GeV}/c$ there are $\frac{2}{3}$ as many standard deviations). The polarization of the τ 's has a large impact on these results. b) The statistical significance of the H^+ peak (dashes) in the two-non- b -jet invariant mass distribution as a function of $\tan \beta$. We assume one SSC year of running and have taken $m_t = 250 \text{ GeV}/c^2$ and $m_{H^+} = 150 \text{ GeV}/c^2$. The upper labels give the $t \rightarrow H^+ b$ branching ratio, which reaches a minimum at $\tan \beta \approx 8$, see fig. 12.

from universality is given in Fig. 13 where we have used the resolutions and efficiencies of [t] the Solenoidal Detector Collaboration (SDC). It is critical to keep track of the polarization of the τ 's; ignoring the polarization reduces the number of standard deviations by a factor of two. Requiring five sigma above background, we conclude that after one year of SSC running one could detect the presence in top decays of the charged Higgs boson decaying to τ 's for all $\tan \beta > 0.5$. For smaller values of $\tan \beta$, where $B(H^+ \rightarrow \tau \nu)$ becomes small, we must employ the $H^+ \rightarrow c \bar{s}$ decay mode.

In Method 2 we have extended the technique described in the SDC EOI [9] to study a $250 \text{ GeV}/c^2$ top quark decaying to H^+ (or W^+) with $H^+(W^+) \rightarrow u \bar{d}$ or $c \bar{s}$. Using ISAJET, jets are formed by clustering final-state particles appearing in the region $|\eta| < 3.0$ within a cone of radius $R < 0.7$. The 4-momenta of the c jets are then smeared with the assumed jet resolution of the SDC calorimeter.

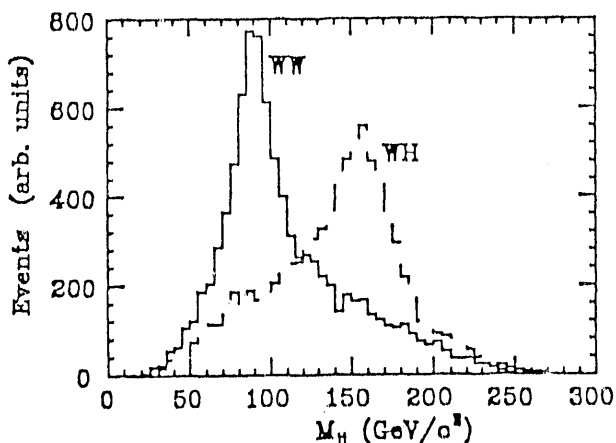


Figure 14: Two-jet mass distribution, for $t\bar{t} \rightarrow WWb\bar{b}$ events (solid) and $t\bar{t} \rightarrow WHb\bar{b}$ events (dashed). Only one two-jet combination per event is plotted: the combination with the two highest p_t non- b jets consistent with the t mass (see text).

Any two non- b jets within $|\eta| < 2.5$ and $p_t > 20$ GeV/ c are then used to form invariant mass combinations. The combinatoric background can be reduced by demanding that these two jets in combination with one of the tagged b jets combine to yield a net three-jet invariant mass smaller than 400 GeV/ c^2 , so as to be consistent, within errors, with the top quark mass $m_t = 250$ GeV/ c^2 . We are assuming that the t mass will already have been measured by the as discussed above. Next we restrict our dijet invariant mass plot to the two (non- b) jets with highest transverse momenta that are consistent with $m(3\text{-jet}) < 400$ GeV/ c^2 . The combinatoric background is severely reduced by only plotting one combination per event, and the above choice is usually the correct one. The resulting peaks due to W^+ and H^+ are shown in Fig. 14.

To quantify the statistical significance of the H^+ mass peak, we again plot the number of standard deviations above background as a function of $\tan\beta$ in Fig. 13. If we require a 5 standard deviation effect, detection of the charged Higgs is straightforward for $0.2 < \tan\beta < 2$. For $\tan\beta > 2$ only the W peak is visible. For $\tan\beta < 0.2$, where there are very few WW decays, the W mass peak is not visible above the background, though the H^+ peak (with 10,000 events for $\tan\beta = 0.2$) is still significant.

In conclusion, we have examined charged Higgs boson production in $t\bar{t}$ events in which one t decays to $H^\pm b$ and the other to $W^\pm b$. In the particular case of $m_t = 250$ GeV/ c^2 and $m_{H^\pm} = 150$ GeV/ c^2 , detection

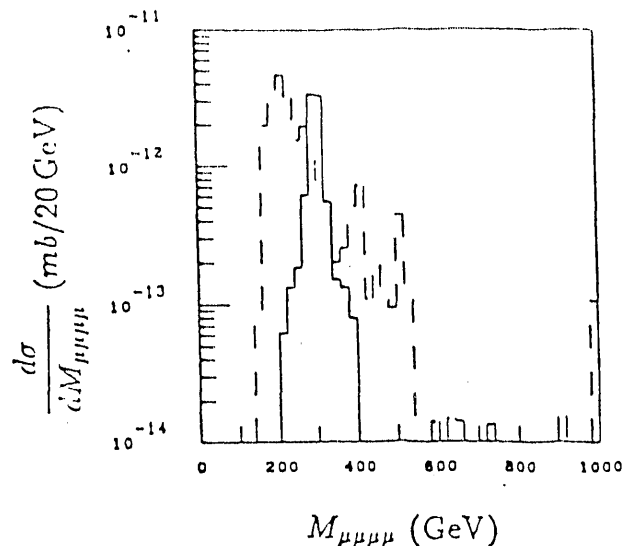


Figure 15: $d\sigma/dM_{\mu\mu\mu\mu}$ vs. $M_{\mu\mu\mu\mu}$ for $\mu^+\mu^-$ pairs with $M_{\mu\mu} = m_Z \pm 20$ GeV. Solid: Higgs, $m_H = 300$ GeV; dashed: $t\bar{t}$ background for $m_t = 200$ GeV.

of the charged Higgs boson will be possible over the entire interesting range of parameter space using either $H^+ \rightarrow \tau\nu$ decays or $H^+ \rightarrow c\bar{s}$ decays or both.

6 Top Decays as Background for Higgs Bosons

While the design luminosity of the SSC is 10^{33} cm $^{-2}$ sec $^{-1}$, it seems likely that luminosity up to 10^{34} cm $^{-2}$ sec $^{-1}$ will be available.[10] This gives an average of 16 interactions per bunch crossing for a 100 mb inelastic cross section. The simplest detector to utilize such high luminosity is one which absorbs all the hadrons and looks only at muons. We study the $t\bar{t}$ backgrounds to Higgs signatures in such a detector. We find that the backgrounds are significant if the $Z^0 \rightarrow \mu^+\mu^-$ mass resolution is poor; one needs either a Z^0 mass resolution significantly better than ± 20 GeV or the ability to make isolation cuts on the muon or both.

Having a fast calorimeter in addition to the muon detector not only would permit such isolation cuts but also might allow one to detect $Z^0 \rightarrow e^+e^-$, potentially increasing the detectable rate for by a factor of four. A very preliminary study suggested that only minimal electron identification is required, [11] so a detector for both electrons and muons may be feasible. We hope to study this possibility in the future.

We have chosen Higgs masses of 300 GeV and 800 GeV, the former because it is close to the $Z^0 Z^0$

threshold and the latter because it is about the upper limit for a well defined resonance. Perturbative unitarity sets an upper limit on m_H of about 1 TeV. Nonperturbative studies [12] of the Higgs gauge-boson system on a lattice suggest an upper limit on the Higgs mass of about 650–700 GeV, but this limit depends to some extent on assumptions and so is not very precise.

A background for $H \rightarrow \mu^+ \mu^- \mu^+ \mu^-$ from a $t\bar{t}$ event requires four semileptonic decays. These can arise in a variety of ways, but we expect that the dominant contribution will come from the decay chain

$$t \rightarrow \mu^+ \nu b \rightarrow \mu^+ \nu \mu^- \bar{\nu} c$$

plus its charge conjugate. We therefore generated 1000 events in each of the five p_T ranges, forcing these decays and including in the cross section a combined semileptonic branching ratio of 10^{-4} . At least for $m_t = 200$ GeV the Monte Carlo statistics approach those for a standard SSC year at low p_T , and they are substantially greater at high p_T .

We have calculated the masses of all pairs of opposite-sign muons with $p_{T,\mu} > 5$ GeV and selected the two pairs with masses closest to the Z^0 mass. We then required that both pairs satisfied

$$M_{\mu\mu} = m_Z \pm 20 \text{ GeV}.$$

Again, this roughly matches the resolution of an iron toroid. In Fig. 15 and Fig. 16 we display the resulting signal and background for the two Higgs and the two top masses. In all cases except for a light top with a heavy Higgs the background is comparable to the signal. This is dramatized by plotting the sum of the signal and the background, which is shown in Fig. 17 and Fig. 18. While there is a dip between the signal peak and the background, it is not very significant at standard SSC luminosity: 10^{-13} mb corresponds to one event per year.

For the $t\bar{t}$ background to the Higgs signal two of the leptons come from b quarks and so are not in general isolated. We therefore expect that applying the isolation cut for each lepton will significantly reduce the background. This is the case but there is still background in the case of a light Higgs and a light top quark, which is not unexpected since the b jet is soft in this case and can give isolated muons. While we have not included resolution, pileup, or electronics noise in making this cut, we have made the cut at a rather high value of E_T in a small cone, so we do not expect these effects to be very important. But clearly this needs more study.

The Higgs background is proportional to the square of the window allowed for a Z^0 and so improves rapidly

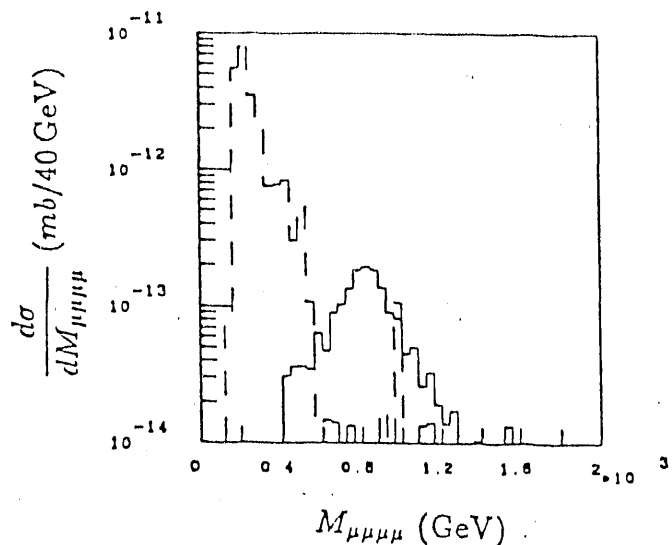


Figure 16: $d\sigma/dM_{\mu\mu\mu\mu}$ vs. $M_{\mu\mu\mu\mu}$ for $\mu^+ \mu^-$ pairs with $M_{\mu\mu} = m_Z \pm 20$ GeV. Solid: Higgs, $m_H = 800$ GeV; dashed: $t\bar{t}$ background for $m_t = 200$ GeV.

with the $\mu^+ \mu^-$ resolution. Thus rejecting the background by a combination of better resolution and isolation cuts appears possible. The $t\bar{t}$ background only excludes the crudest approach to high-luminosity Higgs physics.

7 Aspects of Heavy Quark Neutral Currents

Historically, neutral-current flavor-changing processes have played an important role in the development of the theory of weak interactions. It would be natural to expect that the decays of the top quark, such as $t \rightarrow c\gamma$, could, when discovered, provide not only a detailed test of our understanding of the Standard Model (particularly of the mixing structure), but may also be sensitive to new physics beyond the Standard Model.

However, with the current CDF limit on the top quark mass, a difficulty arises in that the top will decay dominantly within its own generation ($t \rightarrow bW$) with an overwhelming semi-weak rate; consequently, one expects that other channels, including those involving flavor-changing neutral currents, will possess only feeble branching ratios.

A heavy top mass raises some interesting new issues in connection with the flavor changing electromagnetic vertex. Flavor changing radiative decays of light quarks, such as $b \rightarrow s\gamma$ have been the subject of intensive investigation.[13] The conventional approach

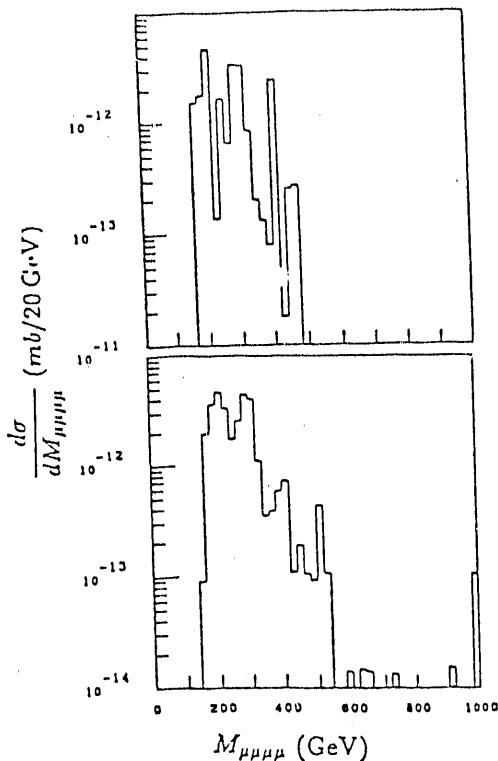


Figure 17: $d\sigma/dM_{\mu\mu\mu\mu}$ vs. $M_{\mu\mu\mu\mu}$ for the sum of the Higgs signal ($m_H = 300$ GeV) and $t\bar{t}$ background. Top graph: $m_t = 100$ GeV. Bottom graph: $m_t = 200$ GeV.

to such neutral current vertices has been to exploit the large mass of the top quark as an *internal* particle, in order to evade the suppression of the neutral current due to the GIM mechanism.[14] By contrast, little is apparently known about the behavior of the flavor-changing electromagnetic vertex when the mass of an *external* particle becomes large compared to M_W . The question naturally arises as to how the GIM mechanism might be modified in this case. In fact, the vertex receives a significant enhancement, at least to one-loop order. The origin of this enhancement is completely different from the case where the mass of an *internal* particle becomes large, and has to do with the onset of physical thresholds in the internal loop integration.[15] Despite the significant enhancement, the rate for $t \rightarrow q\gamma$ is still very small, at least to one loop order.

An interesting scenario is motivated by the large mass of the top, in that the top may provide an effective window to new physics such as coupling to new fermions, SUSY partners, multi-Higgs extensions to the Standard Model, and so on. Specifically, one-photon-exchange Primakoff production [16] of the top, in a sufficiently energetic pp , $\bar{p}p$, or ep collider at small

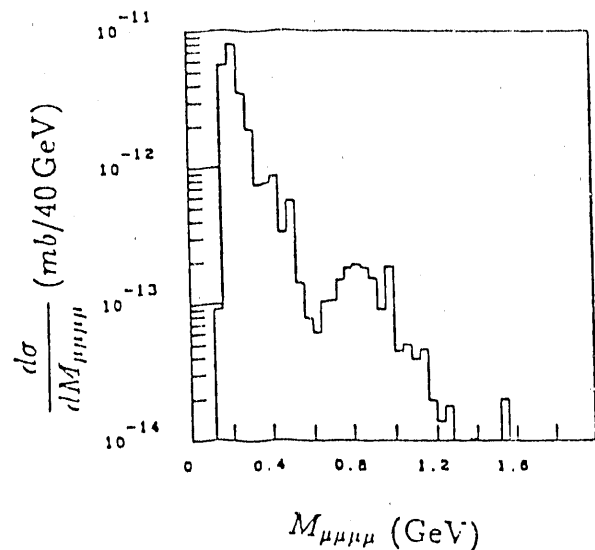


Figure 18: $d\sigma/dM_{\mu\mu\mu\mu}$ vs. $M_{\mu\mu\mu\mu}$ for the sum of the Higgs signal ($m_H = 800$ GeV) and $t\bar{t}$ background for $m_t = 200$ GeV.

q^2 , could yield valuable constraints on new physics.[17] The cross section for top production through this mechanism is much larger than one might have expected. Whereas at fixed s , sufficiently above the top production threshold, the gluon fusion cross-section falls off as a power of m_t , the Primakoff cross-section could actually increase with m_t for a range of masses. In a two-Higgs extension of the Standard Model, with four generations of quarks, the Primakoff process could provide useful constraints on certain sectors of the parameter space of the model.

8 Conclusions

There is an excellent prospect that the top quark will be discovered in data from forthcoming runs of the Tevatron. The characteristics of top can be well studied at the SSC or LHC. Eventually the greatest interest in top production may be as a background to other physics, but the implications of the high mass of the top quark may lead in unexpected directions.

9 References

- [1] A. Barbaro-Galtieri, talk at this Snowmass meeting.
- [2] V. Barger, J.L. Hewett, and T.G. Rizzo, *Physical Review Letters* **65**, 1313 (1990).
- [3] *Workshop on Physics at Fermilab in the 1990's*, edited by Dan Green and Henry Lubatti, (Breck-

enridge, CO, 1990).

- [4] B. Hubbard, SDC Note SSC-SDE-31 (unpublished).
- [5] Private communication from Edward Wang.
- [6] D. Decamp *et al.*, *Phys. Lett.* **B244**, 551 (1990).
- [7] F.J. Gilman and R.P. Kauffman, *Phys. Rev.* **D37**, 2676 (1988).
- [8] R.M. Barnett, J.F. Gunion, H.E. Haber, I. Hinchliffe, B. Hubbard and H.-J. Trost, in the Higgs section of these proceedings; other references are given there.
- [9] Expression of Interest submitted by the Solenoidal Detector Collaboration to the SSC Lab, May 1990.
- [10] A. Chou, *Possible Scenario to Reach Higher Luminosities*, SSC-N-684 (1989).
- [11] F.E. Paige, *Int. J. Mod. Phys.* **A2**, 993 (1987).
- [12] J. Kuti, L. Lin, and Y. Shen, *Phys. Rev. Lett.* **61**, 678 (1988).
- [13] For example see B. Grinstein *et al.*, *Phys. Lett.* **B 202**, 138 (1988); R. Grigjanis *et al.*, *Phys. Lett.* **B 213**, 355 (1988) and **B 224**, 209 (1989).
- [14] S. Glashow, J. Iliopolis, and L. Maiani, *Phys. Rev.* **D2**, 1285 (1970).
- [15] B. Dutta Roy *et al.*, *Phys. Rev. Lett.* **65**, 827 (1990). See also P. Krawczyk, *Z. Phys.* **C44**, 509 (1989); G. Eilam, B. Haeri and A. Soni, *Phys. Rev.* **bf D41**, 875 (1990); and W.-S. Hou and R. G. Stuart, CERN preprint TH 5686/90 (unpublished).
- [16] H. Primakoff, *Phys. Rev.* **81**, 809 (1951); A. Halprin, C. M. Anderson and H. Primakoff, *Phys. Rev.* **152**, 1295 (1966).
- [17] B. Dutta Roy *et al.*, *Phys. Rev. D* (to be published).

DISCLAIMER

This report was prepared as an account of work sponsored by an agency of the United States Government. Neither the United States Government nor any agency thereof, nor any of their employees, makes any warranty, express or implied, or assumes any legal liability or responsibility for the accuracy, completeness, or usefulness of any information, apparatus, product, or process disclosed, or represents that its use would not infringe privately owned rights. Reference herein to any specific commercial product, process, or service by trade name, trademark, manufacturer, or otherwise does not necessarily constitute or imply its endorsement, recommendation, or favoring by the United States Government or any agency thereof. The views and opinions of authors expressed herein do not necessarily state or reflect those of the United States Government or any agency thereof.

END

DATE FILMED

12 / 17 / 90

